



## CHAPTER IV

### RESULTS AND DISCUSSION

This chapter discusses about the effects of the catalyst mixing (KL and Y zeolite) with various ratios and the packing sequence, and about also the effects of noble metal on the quality and quantity of oils and others products.

The catalytic pyrolysis of scrap tires was carried out with the two zeolites packed in the reactor (the upper zone) in the double bed manners. The effects of the weight fraction of KL ( $\emptyset_{KL}$ ), was varied (0, 0.25, 0.5, 0.75, and 1).

$$\emptyset_{KL} = \frac{W_{KL}}{W_{KL} + W_Y} ; \emptyset_Y = 1 - \emptyset_{KL}$$

For the each packing style, the notations; Y + KL, Y ---> KL, and KL ---> Y represent the physical mixture of Y and KL zeolites, Y placed in the first layer then KL, and KL placed in the first layer then Y, respectively (see Figure 3.1).

#### 4.1 Catalyst Characterization

##### 4.1.1 Crystal Structure of the Catalysts

The XRD patterns of physical mixtures without and with platinum loading are shown in Figure 4.1. The characteristic peaks of Y ( $\emptyset_{KL} = 0$ ) and KL zeolites ( $\emptyset_{KL} = 1$ ) are almost unchanged, indicating that Y and KL still retained their crystalline structure. With the increased weight fraction of KL, the characteristic peaks of Y zeolite at 5.60°, 11.80°, 14.75°, 19.35°, 22.70°, 24.35°, 25.60°, 27.15°, 28.05°, 29.15°, 30.75°, and 33.75° slightly appear at the fractions  $\emptyset_{KL} = 0.25$  and 0.5, indicating that the zeolite Y contributes with small amount of zeolite KL. Then, when the weight fraction is increased to  $\emptyset_{KL} = 0.75$ , the characteristic peaks of KL zeolite are more dominant. Moreover, The signal for the five main characteristic peaks of crystalline platinum ( $2\theta = 39.7^\circ, 46.3^\circ, 67.5^\circ, 81^\circ, \text{ and } 81.5^\circ$ ) are not observed. Probably, the amount of platinum loading is below the detectable range of the XRD equipment.

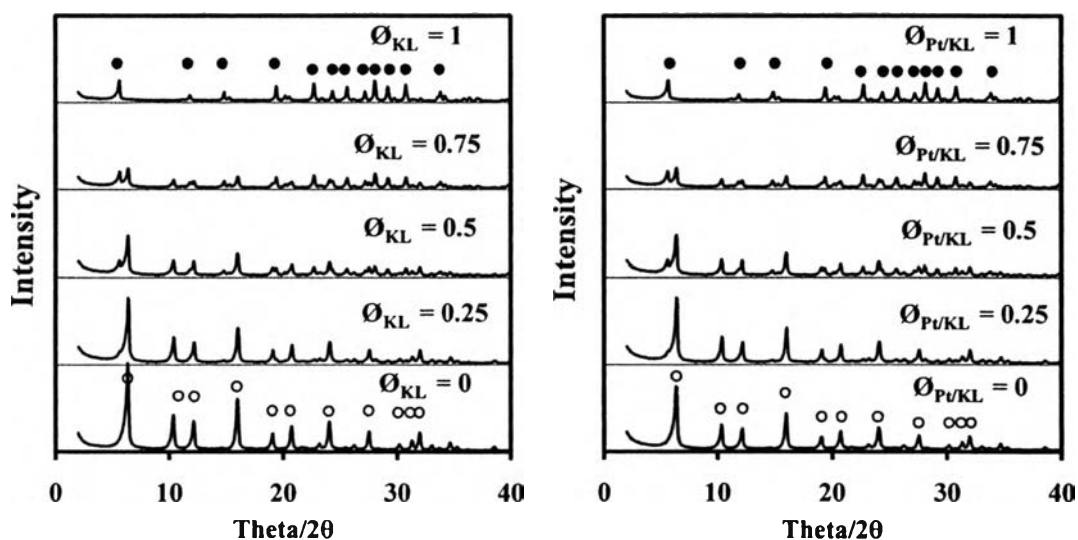


**Figure 4.1** XRD patterns of (a) physical mixtures (Y + KL) and (b) physical mixtures with platinum loading (Pt/Y + Pt/KL) at various weight fractions of KL (opaque circles represent the characteristic peaks of KL zeolite, and open circles represent the characteristic peaks of Y zeolite)

#### 4.1.2 Physical Properties and Catalytic Activities

Physical properties and acid strength in the case of Y and KL physical mixtures, without and with platinum loading are summarized in Table 4.1. The BET surface area of pure Y and KL is about 296.7 and 578.2 m<sup>2</sup>/g, respectively. However, the BET surface area in the case of the platinum loading is found to be relatively low, about 265.1 and 559.7 m<sup>2</sup>/g. This is an expected result, since the surface and pores of zeolite are covered by platinum metals during the impregnation step. Also, the significant reduction of the pore volume is observed after the impregnation step. Acid and Basic strength of the physical mixture case were measured using Hammett indicators. As can be seen from Table 4.1.  $H_0$  of KL zeolite is between 7.2–8.2, indicating the formation of strong basic sites on its surface. The rest of catalysts are found to be amphoteric with a site strength ( $H_0$ ) in the range of 0.8 and 7.2. Y, Pt/Y, and the physical mixtures at  $\text{Ø}_{\text{KL}} = 0.25$  exhibit a higher acid strength ( $0.8 < H_0 \leq 3.3$ ) than other catalysts. Moderately strong acid strength ( $3.3 < H_0 \leq 4.8$ ) belongs to physical mixtures at  $\text{Ø}_{\text{KL}} = 0.5$  and 0.75. And, the weak one ( $4.8 < H_0 \leq 7.2$ ) is Pt/KL.

**Table 4.1** Physical properties and acid strength of all physical mixtures

Catalyst	Pt (wt%)	Surface area (m <sup>2</sup> /g)	Pore volume (cm <sup>3</sup> /g)	Acid/Base site strength, ( $H_0$ )
Y	-	578.2	0.58	$0.8 < H_0 \leq 3.3$
$\emptyset_{KL} = 0.25$	-	507.8*	0.53*	$0.8 < H_0 \leq 3.3$
$\emptyset_{KL} = 0.5$	-	437.5*	0.49*	$3.3 < H_0 \leq 4.8$
$\emptyset_{KL} = 0.75$	-	367.1*	0.44*	$3.3 < H_0 \leq 4.8$
KL	-	296.7	0.39	$7.2 < H_0 \leq 8.2$
Pt/Y	0.98	559.7	0.51	$0.8 < H_0 \leq 3.3$
$\emptyset_{Pt/KL} = 0.25$	-	486.1*	0.47*	$0.8 < H_0 \leq 3.3$
$\emptyset_{Pt/KL} = 0.5$	-	412.4*	0.42*	$3.3 < H_0 \leq 4.8$
$\emptyset_{Pt/KL} = 0.75$	-	338.8*	0.38*	$3.3 < H_0 \leq 4.8$
Pt/KL	0.99	265.1	0.33	$4.8 < H_0 \leq 7.2$

\* By calculation

## 4.2 Effect of Double Beds on Pyrolysis Products

### 4.2.1 Pyrolysis Yields

The product yields are reported in terms of the gas to oil ratio as shown in Figure 4.2. The results presented in the figure include the non-catalytic case and each of pure zeolite cases. It can be seen that the gas-to-liquid ratio (G/L) of all double bed cases is higher than the pure zeolite cases. Similar product yields results have been reported by Shen *et al.*, 2006, on which the presence of USY zeolite served to reduce the oil yield and then increase the gas yield, with the formation of coke on the catalyst. They suggested that the low Si/Al ratio of USY catalyst resulted in high surface activity. Thus, it is clear that there are more reactants available to be cracked into the gaseous fraction. Moreover, for KL  $\rightarrow$  Y and Y + KL, the G/L ratio passes through the maxima at  $\emptyset_{KL} = 0.75$ , and then decreases as the amount of KL zeolite increases. For Y  $\rightarrow$  KL, the G/L ratio dramatically increases with the increasing amount of KL, reaching the maximum at  $\emptyset_{KL} = 0.5$ , and then decreases at

$\phi_{KL} = 0.75$ . Consequently, the physical mixture at  $\phi_{KL} = 0.75$  exhibits the best performance in terms of the G/L ratio as compared to the two packing sequences.

Moreover, for the double bed cases, the physical mixture (Y + KL) produced the higher amount of lower molecular weight products than the packing sequences cases (Y  $\rightarrow$  KL and KL  $\rightarrow$  Y). When the upper layer was charged with Y zeolite, the catalytic product from the lower layer can be protonated, which forms carbenium ions, followed by cracking into the gaseous fraction. Besides, when the catalyst was reversed, the gaseous fractions are also increased via carbanions from KL zeolite. However, the G/L ratio of the physical mixtures is the highest as compared to the two cases of layer-style packing. The solid yield remains almost constant throughout all experiments at around 44% (not shown in the figure), which means that the tire rubber is completely decomposed at 500 °C.

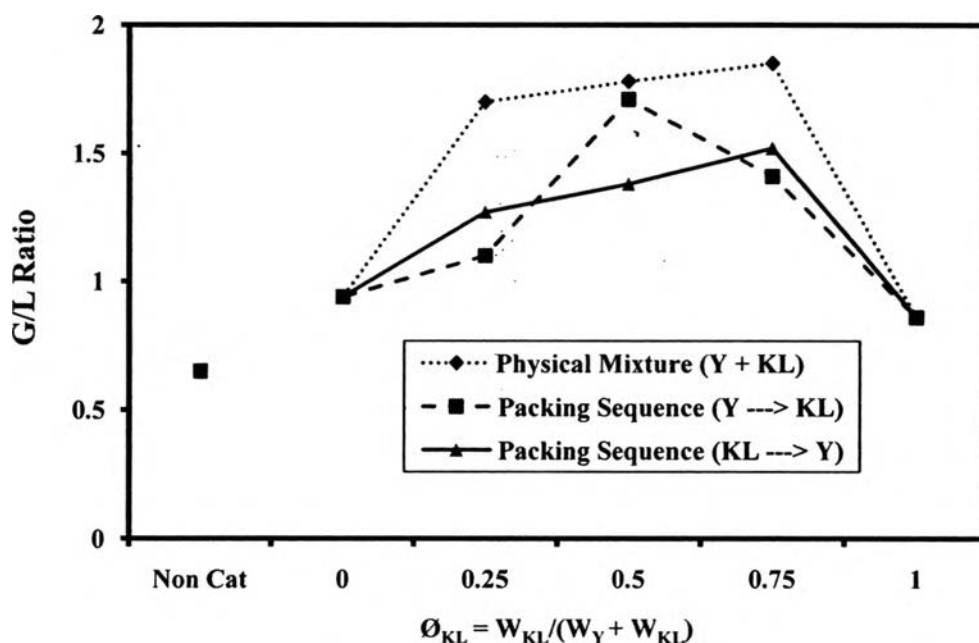


**Figure 4.2** G/L ratio at different packing sequences and various weight fractions of KL.

#### 4.2.2 Gas Composition

Typically, the components of gas produced from pyrolysis consist of methane, ethylene, ethane, propylene, C<sub>4</sub>-, C<sub>5</sub>- C<sub>6</sub>- C<sub>7</sub>- and C<sub>8</sub>-hydrocarbons together with some CO, CO<sub>2</sub> and SH<sub>2</sub> (Jitkarnka *et al.*, 2007 and Rodriguez *et al.*, 2001). As observed in Figure 4.3, the main compositions of the gaseous fraction are also hydrocarbon gases such as methane, ethane, ethylene, propylene, and mixed C<sub>4</sub>-C<sub>8</sub>. The yield to gaseous fractions of physical mixing case and the two cases of layer-style packing are much higher than the non-catalytic and the catalytic pyrolysis using the pure Y and KL zeolites. Especially, the physical mixture (Y + KL) at the  $\emptyset_{KL} = 0.25$  gives tremendously high mixed-C<sub>4</sub> products. And the other two physical mixtures at  $\emptyset_{KL} = 0.5$  and 0.75 also provide the high mixed-C<sub>4</sub> products. It can be explained that the primary products obtained from catalytic pyrolysis are further cracked to light gas products. For the case of packing sequence, the data are shown in Appendix C because these two cases (Y---> KL and KL ---> Y) show the same trend as compared to the physical mixing case (Y + KL).

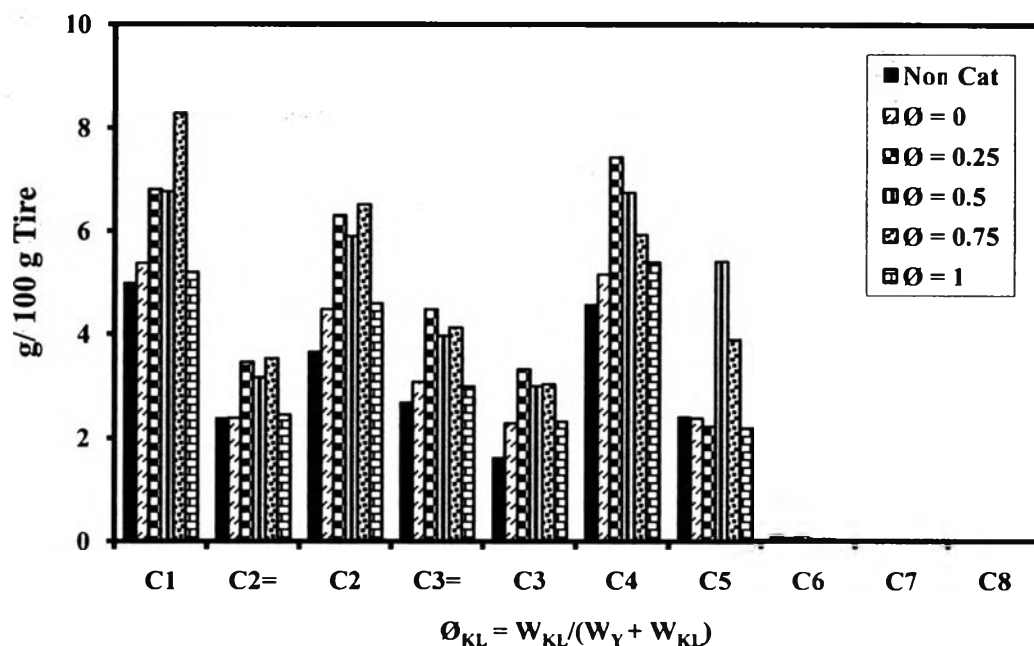


**Figure 4.3** Distribution of gas compositions for the case of physical mixtures of Y and KL zeolites.

#### 4.2.2.1 Light Olefin and Cooking Gas Production

Light olefins and cooking gas are well known as the most important commercial products in many industries. From the results, it is clear that the yields of the light olefins and cooking gas obtained from all double bed cases are higher than the non-catalytic case and the catalytic pyrolysis with pure zeolites ( $\emptyset_{KL} = 0$  and 1) as shown in Figures 4.4–4.5. This can be suggested that the different properties of the two catalysts in terms of their acidic and basic surfaces can possibly influence the production of gases. However, the physical mixing case of  $\emptyset_{KL} = 0.25$  is the best catalyst to produce apparently a high amount of propane with a considerable amount of C4 hydrocarbons, which is, thus, the best choice to produce cooking gas (60% propane and 40% mixed-C<sub>4</sub>). Moreover, it is found that this weight fraction also provides a high amount of ethylene and propylene. Hence, the physical mixture at the  $\emptyset_{KL} = 0.25$  could be the best catalyst combination to produce light olefins as well.

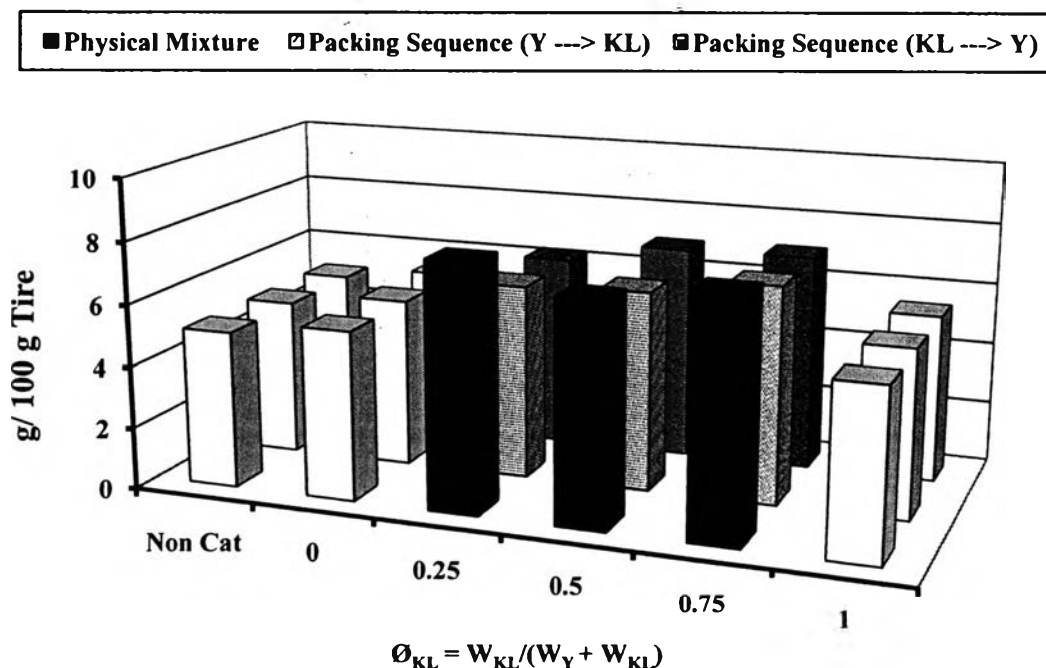


**Figure 4.4** Effects of double bed packing and the weight fraction of KL on light olefins production.

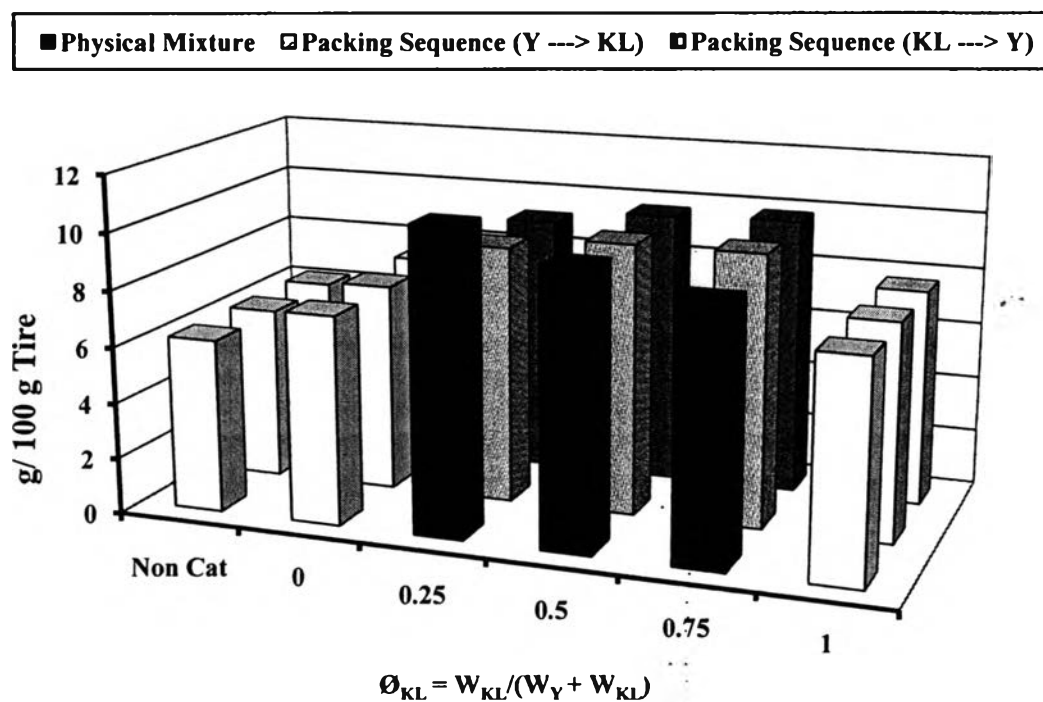


**Figure 4.5** Effects of double bed packing and the weight fraction of KL on cooking gas production.

#### 4.2.3 Oil Products

The oils derived from catalytic pyrolysis were analyzed by using a SIMDIST Gas Chromatography (SIMDIST). Each fraction was classified according to its boiling point range, which are naphtha (<200 °C), kerosene (200–250 °C), light gas oil (250–300 °C), heavy gas oil (300–370 °C), and long residue (>370 °C) (Düng, 2009).

The effects of using the two zeolites simultaneously packed in the reactor in two opposite orders on the quantity of petroleum fractions are illustrated in Figures 4.6–4.8. The results show that the two catalysts with various packing ratios strongly affect the amount of naphtha. For example, the physical mixture (Y +KL) at  $\varnothing_{KL} = 0.75$  gives the highest yield of naphtha (~ 48%) and also the lowest yields of residue (~ 4%) among the other mixtures as shown in Figure 4.6. This can be suggested that all double bed cases have higher cracking activity than using each separate zeolite, resulting in the higher yield to naphtha fraction. However, kerosene

and LGO are still present in the lowest yield at  $\phi_{KL} = 0.25$  and  $0.75$  when compared to a pure single zeolite.

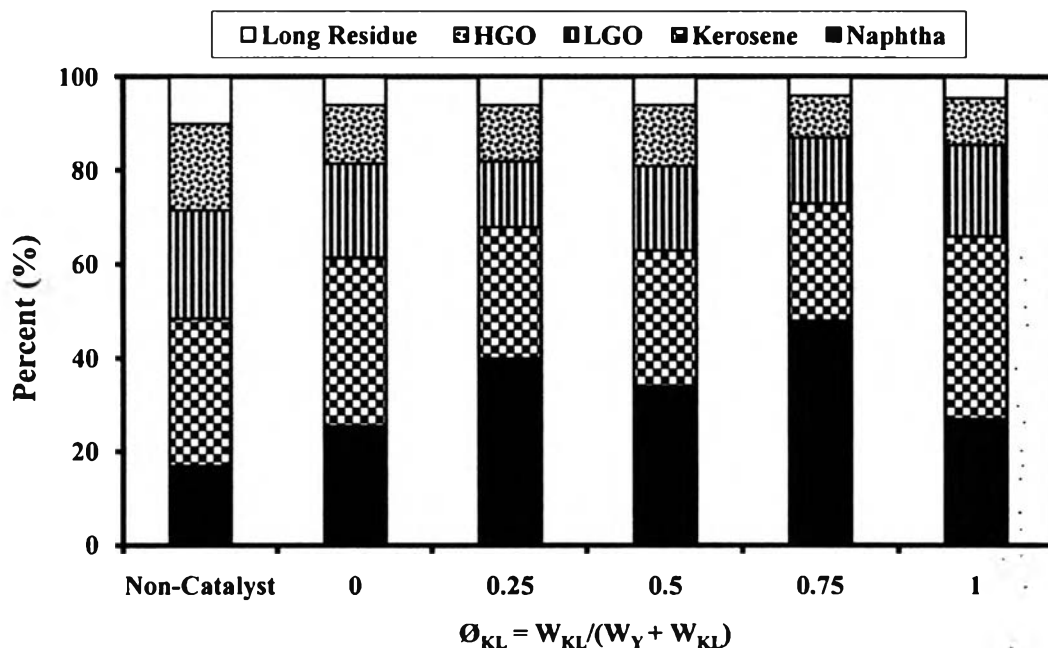


**Figure 4.6** Effect of physical mixing (Y + KL) on petroleum fractions in maltenes.

Figure 4.7 shows the overall quantity of the main petroleum product obtained from various weight fractions for the case of Y  $\rightarrow$  KL. It can be clearly seen that the quantity of naphtha increases with the increasing amount of KL zeolite. However, when the amount of KL zeolite in the layer-style packing is higher than 0.5, naphtha starts to decrease. Contrarily, kerosene starts to increase when the amount of KL zeolite reaches the  $\phi_{KL} = 0.5$ . This is probably due to a sufficient decomposition of heavy molecules in the KL top layer via carbanion intermediates. Moreover, Y zeolite in the first layer still mainly catalyzes cracking of large molecules via the formation of carbenium ion intermediate by the protonation of heavy olefins and cyclization is a minor reaction.



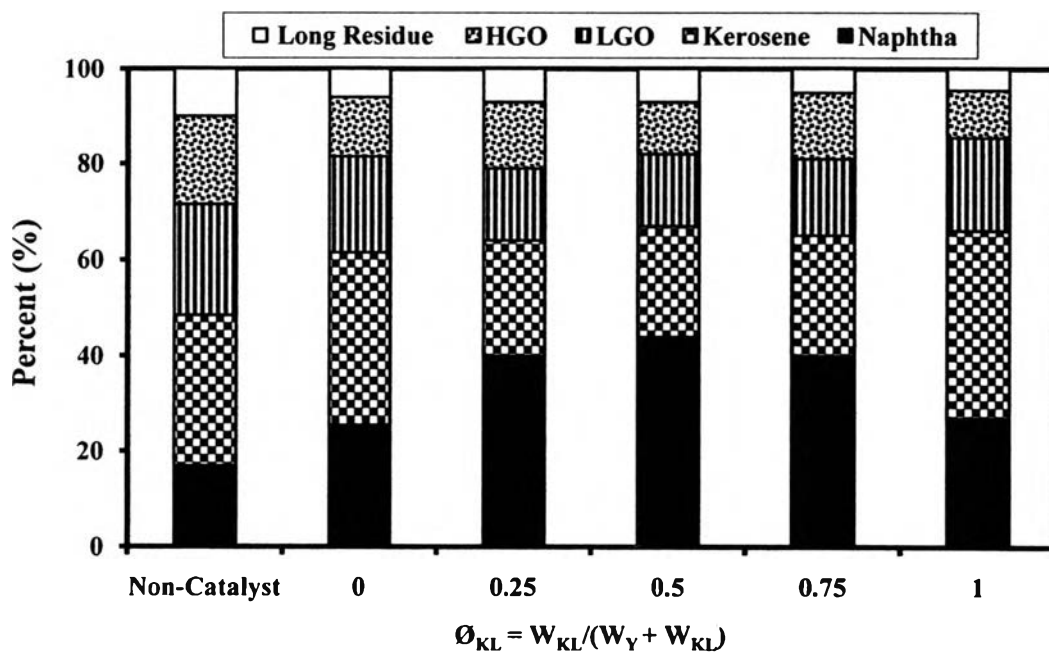


**Figure 4.7** Effect of packing sequence (Y ---> KL) on petroleum fractions in maltenes.

For the effect of weight fraction for the cases of KL ---> Y on the quantity of petroleum fractions, as the KL zeolite addition in the first layer of packing catalyst increases, the yields to kerosene and LGO are decreased whereas the yields to naphtha and HGO are increased as shown in Figure 4.8. Moreover, pure KL zeolite gives the highest yield of kerosene and the lowest yields HGO. Thus, the use of Y zeolite as a second layer can enhance the cracking activity via Brönsted sites or carbenium ion intermediates followed by cracking into small fractions like naphtha.

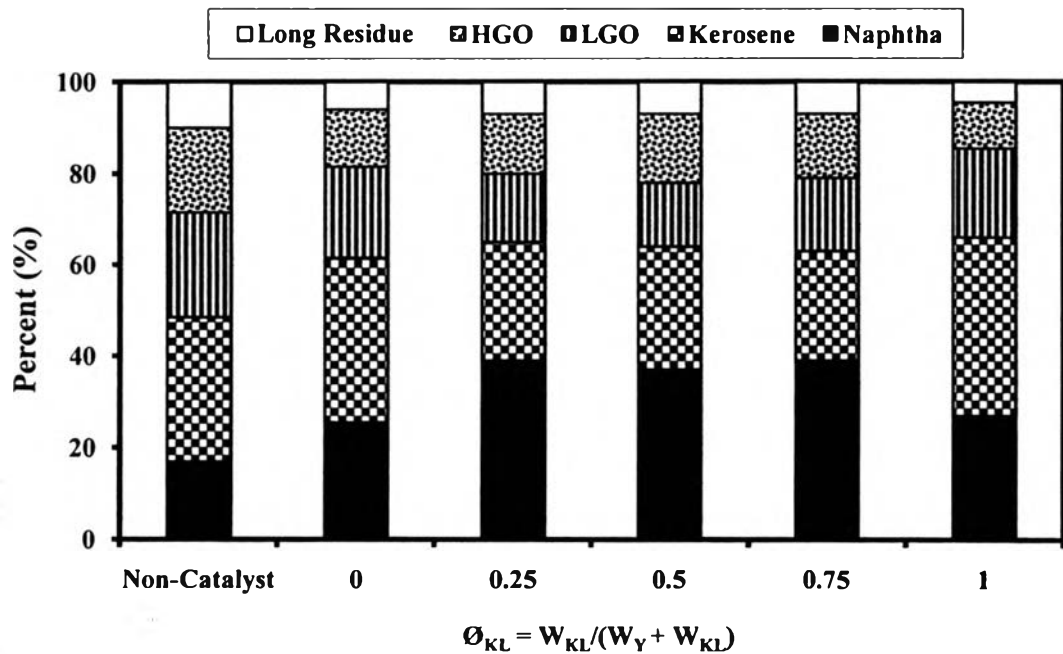


**Figure 4.8** Effect of packing sequence (KL  $\rightarrow$  Y) on petroleum fractions in maltenes.

In conclusion, all the double bed catalysts give a high yield of cooking gas, light olefins, and naphtha while the two single zeolites (Y and KL) provide the slightly high yields of heavier products such as kerosene and LGO. From these results, it can be explained that the predominant cracking on the physical mixtures (Y + KL) leads mainly to the formation of light hydrocarbon in the range  $C_3-C_6$ . Some overcracking is surmised to occur which explain the enhancement in the gaseous fraction and the decrease in the liquid fraction (Aguado *et al.*, 2001). The same result was found by Ou *et al.* (2006) who studied the performance of ethylene and propylene production from a catalyst consisting of a metal-based component and a solid acid component. The results showed that the mixed catalyst gave a high conversion of ethylene, propylene, and butylenes that are higher than the sum of yields of the individual components. And they also suggested that the natural binary composition have the appropriate acid strength for reaction such as cracking. However, the basic catalyst can also occur in a wide variety of hydrocarbon reactions such as double bond migration, dehydrogenation, hydrogenation, and isomerization via the carbanion intermediate (Hattori, 1995).

In the cases of packing sequence, the second layer with a long enough contact time contributes to secondary reactions, which lead to less oil and more gas product (Dai *et al.*, 2001). Aboul-Gheit *et al.* (2005) suggested that using acidic monofunctional catalysts can enhance dehydrogenation and isomerization on the acid sites leading to the higher amount of light olefins product. And in year 2002, Wakui *et al.* studied the two-stage dehydrogenative of *n*-butane for light olefins production. They found that the *n*-butane was first dehydrogenated to *n*-butene and then converted to ethylene and propylene products. As compared to this work, the thermal degradation of heavy molecules occurs, and the resulted molecules are allowed to isomerize into pore of KL zeolite and cracked into the gaseous or small molecule on the acid catalyst. However, when the catalyst sequence was first Y and then followed by KL (Y  $\rightarrow$  KL), the light olefins and cooking gas production are almost the same as when the upper layer was charged with Y zeolite. This indicates that the order of packing sequence does not have any significant effect on light olefins and cooking gas production. However, in this packing style, the heavy molecules hydrocarbon mixture can be directly cracked on the Y catalyst followed by isomerization (double bond migration) on KL zeolite resulting in the higher yield to naphtha fraction.

The saturated hydrocarbons and aromatic compounds in maltene were analyzed by using liquid column chromatography. Figure 4.9 shows the effect of physically mixed catalysts (Y + KL) on chemical composition in maltene. The results show that the physical mixtures (Y + KL) provide a higher fraction of saturated hydrocarbons and then the lower total aromatic compounds than the pyrolysis using pure zeolites. Moreover, the yield of saturated hydrocarbons is slightly dropped with the increase of KL zeolite from  $\phi_{KL} = 0.25$  to 1. And also the aromatic compounds increase with the amount of KL zeolite addition. Wakui *et al.* (1999) suggested that the Brønsted acid sites and carbanion intermediate from basic sites act as active hydrogenation for alkenes at higher reaction temperature. As a result, the overall reaction is predominated by hydrogenation of heavy hydrocarbon molecules, leading to the large amount of saturated hydrocarbon in maltene fraction.

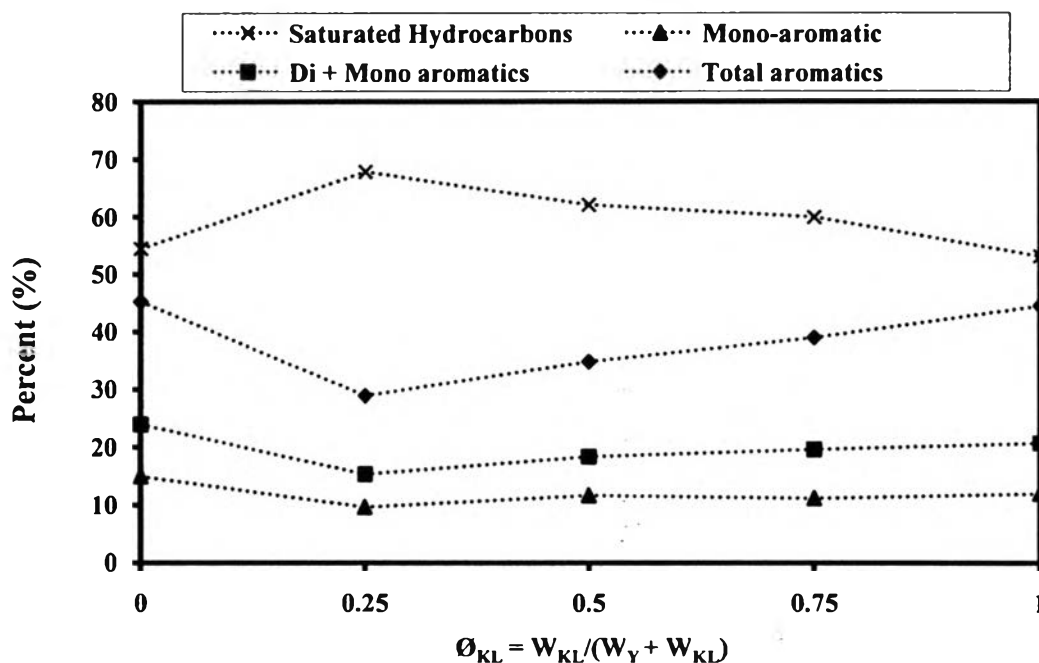


**Figure 4.9** Chemical composition in maltene obtained from the physical mixtures of zeolites (Y + KL) with various weight fractions of KL.

The chemical composition in maltene obtained from packing sequence (Y  $\rightarrow$  KL) with various  $\phi_{KL}$  is shown in Figure 4.10. It is found that mono-aromatics are comparable for all cases. And also the increase in the amount of KL zeolite causes a slight increase in saturated hydrocarbons, which then decreases the total aromatic hydrocarbons as the amount of KL zeolite increases from  $\phi_{KL} = 0$  to 0.25. In addition, the yield to total aromatic hydrocarbons increases with increasing the amount of KL zeolite (from  $\phi_{KL} = 0.25$  to 0.5). The saturated and the total aromatic hydrocarbons are not influenced by the zeolite addition beyond  $\phi_{KL} = 0.5$ . Afterwards, the yields are fairly constant. Because of the high dehydrogenation activity of KL zeolite, this sequence of catalysts produces a significant amount of total aromatic and, hence, the total aromatic is rather high when adding the KL zeolite over  $\phi_{KL} = 0.5$ .

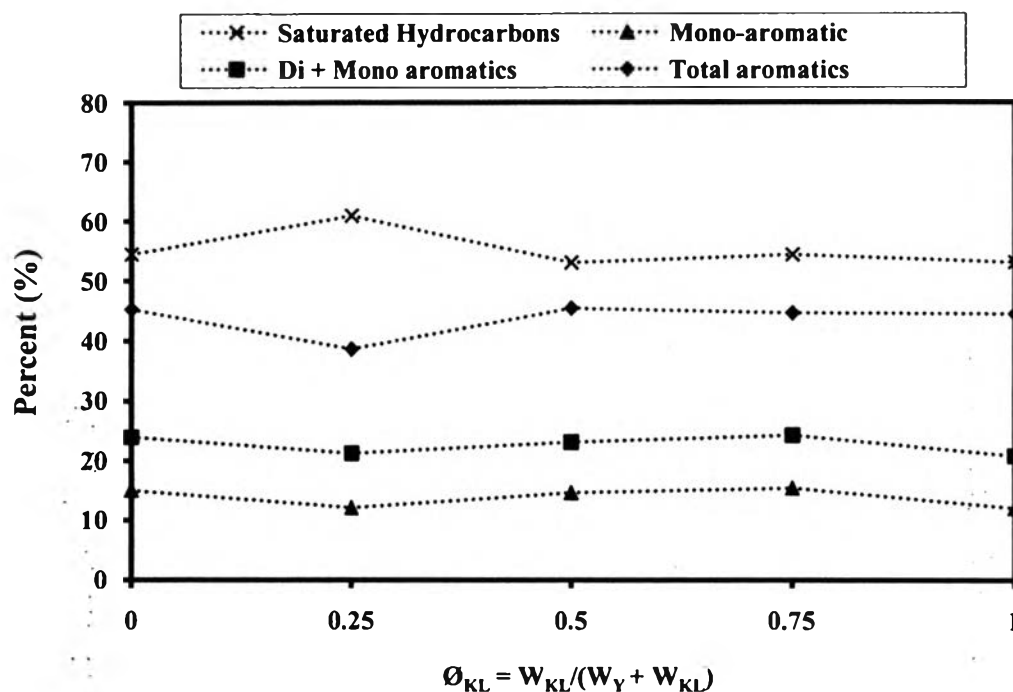


**Figure 4.10** Chemical composition in maltene obtained from the packing sequence (Y  $\rightarrow$  KL) with various weight fractions of KL.

Based on the chemical composition in maltene obtained from packing sequence (KL  $\rightarrow$  Y) in Figure 4.11, the weight fraction of KL affects on the saturated hydrocarbons. The saturated hydrocarbons are decreased with increasing KL zeolite from  $\emptyset_{KL} = 0$  to 0.5. The results of the total aromatic hydrocarbons show a marked increase from 45.3 to 51.9% when the amount of KL zeolite increases from  $\emptyset_{KL} = 0$  to 0.5. Beyond  $\emptyset_{KL} = 0.5$ , the saturated hydrocarbon is increased, but the total aromatic hydrocarbon is decreased when the amount of KL zeolite increases from  $\emptyset_{KL} = 0.5$  to 1. This indicate that the cyclization reactions also occur on the strong acid sites of zeolite to produce a large amount of aromatics at  $\emptyset_{KL} = 0$  to 0.5. Afterwards, the hydrogenation reaction become dominant, leading to the increase of saturated hydrocarbon.

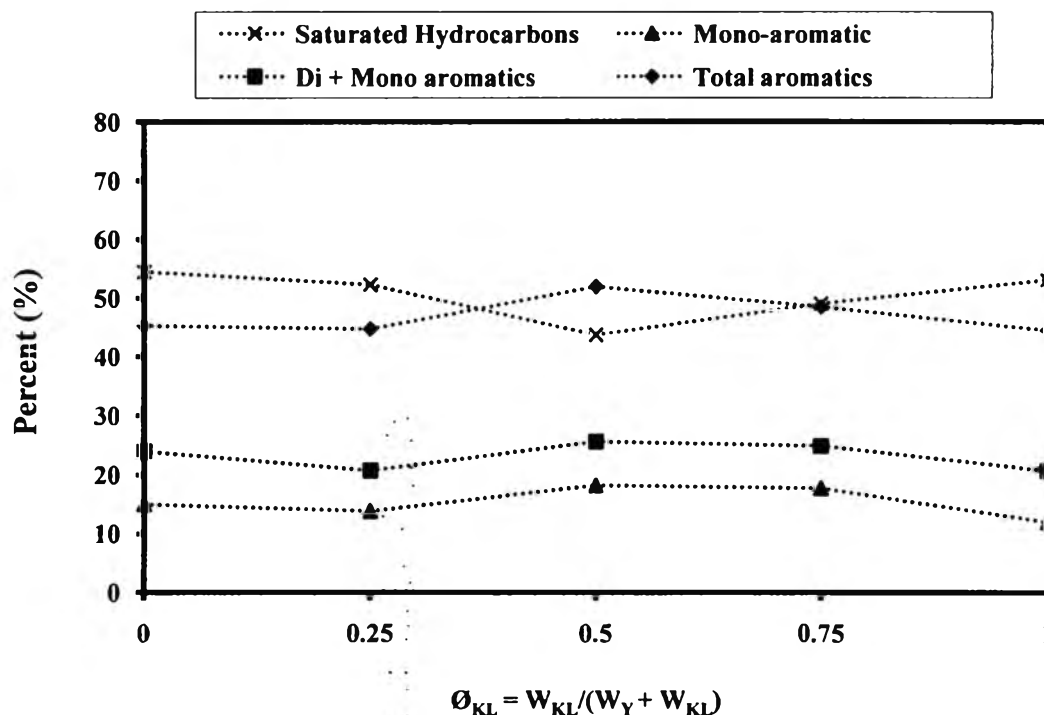


**Figure 4.11** Chemical composition in maltene obtained from the packing sequence (KL ---> Y) with various weight fractions of KL.

The results in this section indicate that that total aromatic (from the two packing sequences, Y ---> KL and KL ---> Y) are formed directly from the light olefins molecules combined to form single ring aromatics, and the single ring aromatics can also combine with another molecules to form bigger molecules such as polyaromatic (Cypres *et al.*, 1987). Therefore, the yield to light olefins of packing sequence cases is less than the physical mixing case (see Figure 4.3). Moreover, in 2005, Fan *et al.* studied a catalyst having excellent olefin reduction activity without a loss in the octane number of gasoline. They suggested that the aromatic hydrocarbon was favored by strong acid sites, especially at high temperatures. However, too many strong acid sites can seriously lower the stability of the catalyst. Therefore, that is the reason why the yield to total aromatics in the case of packing sequence is higher than physical mixture cases. In addition, the physical mixtures give the highest saturated hydrocarbons. It can be assumed that this packing style acquires a modest

hydrogenation activity, as proposed by Kani *et al.* (1992) who assumed that Brönsted acid sites act as active hydrogenation sites for alkenes at high temperatures.

Asphaltene formation is another way to determine the quality of liquid product. The results can be observed in Figure 4.12. The main trend is that all catalysts, especially the physical mixture of  $\phi_{KL} = 0.25$ , can drastically reduce asphaltene in the oil products. It is suggested that the complex molecules of asphaltene are possibly cracked on the active sites of catalysts.

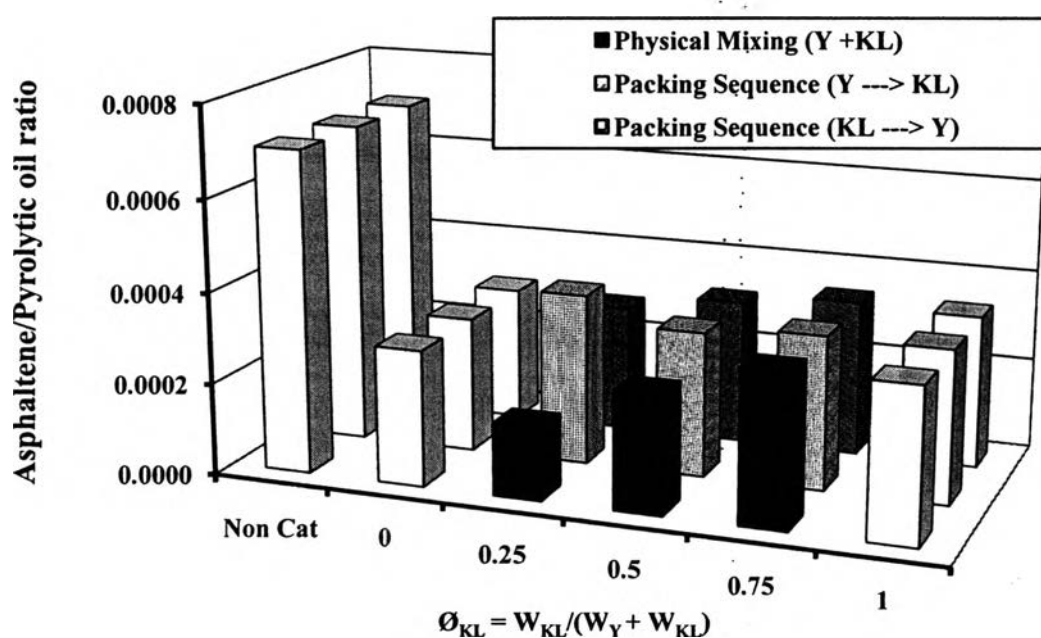


**Figure 4.12** Weight fraction of asphaltene in pyrolytic oils obtained from using the double beds of zeolites.

#### 4.2.4 Coke and Sulfur Formation

The coke formation and sulfur deposition on catalysts are shown in Table 4.2. Typically, coke formation can be produced by two basic mechanisms. First, coke is formed primarily from high molecular weight compounds such as asphaltenes and resins by alkylation-precipitation reactions. The second mechanism produces coke by condensation of poly-aromatic compounds (Chaalal and Roy, 1996). Due to the highest acid strength of Y zeolite; therefore, the amount of coke formation on Y is the higher than KL zeolite even the Y is in the first layer.

However, the physical mixtures (Y + KL) exhibit a high amount of coke deposition. This may be due to the strong acid strength more than the pure zeolites (see Table 4.1), leading to the highest yield of cooking gas and light olefins in Figures 4.4 and 4.5.

Sulfur is one of the most important factors in decreasing the catalyst activity (Fang *et al.*, 1997). The detail results of sulfur analysis for different styles of packing are also summarized in Table 4.2. Most of spent catalysts show a higher amount of sulfur deposited on the second layer than the first layer. Its deposition mostly occurs on the second layer because a large number of sulfur-containing compounds deposit on the catalyst as secondary products. It maybe concluded that the formation of complexes containing sulfur on the surface of catalyst is one of important reasons, resulting in the deactivation of the catalyst.

**Table 4.2** Coke and sulfur formation from the different packing styles without platinum loading

Catalyst	$\emptyset_{KL}$	Layer	Coke (g/g cat)	Sulfur (%)
Y	0	-	0.32	0.51
Physical Mixture (Y + KL)	0.25	-	0.31	0.56
	0.5	-	0.30	0.56
	0.75	-	0.31	0.54
Packing Sequence (Y ---> KL)	0.25	KL	0.18	0.31
		Y	0.20	0.22
	0.5	KL	0.26	0.50
		Y	0.28	0.38
	0.75	KL	0.33	0.60
		Y	0.32	0.48
Packing Sequence (KL ---> Y)	0.25	Y	0.33	0.53
		KL	0.18	0.28
	0.5	Y	0.33	0.59
		KL	0.19	0.31
	0.75	Y	0.43	0.78
		KL	0.18	0.50
KL	1	-	0.29	0.49



### 4.3 Effect of Platinum Loading on Double Bed Catalysts

As well known, the preparation of catalysts with enhanced properties could be achieved in many ways. One of the most interesting ways is impregnation with a metal like platinum. In this experiment, all of the zeolites were loaded with 1.0% platinum metal by incipient wetness impregnation technique before being packed in the same manners as in Section 4.2.

#### 4.3.1 Pyrolysis Yields

Tables 4.3–4.4 show the yields of products at various packing styles of the two zeolites (Y and KL) without and with platinum loading, respectively. It can be seen from Figures 4.13–4.14 that the presence of platinum influences on the yields of gas and liquid products. For the ease of analysis, the ratio ( $\alpha_i$ ) for pyrolysis products is then defined as shown in the following equations:

$$\alpha_i = \frac{\text{Activity, } i \text{ of Pt-load catalyst beds}}{\text{Activity, } i \text{ of same catalyst beds without Pt}}$$

$$\text{For, example; } \alpha_{\text{gas yield}} = \frac{\text{Gas yield of Pt-loaded beds}}{\text{Gas yield of same beds without Pt}}$$

**Table 4.3** Pyrolysis products obtained from the different packing styles of Y and KL zeolites

Case		Product Yield		Yield of Light Olefins (g/100 g Tire)	Yield of Cooking Gas (g/100 g Tire)
Catalyst	$\emptyset_{KL}$	Gas (%)	Liquid (%)		
Pure Y	0	25.3	27.0	5.47	7.45
Physical Mixture (Y + KL)	0.25	34.2	20.2	7.94	10.8
	0.5	35.0	19.7	7.14	9.76
	0.75	35.4	19.1	7.67	8.98
Packing Sequence (Y ---> KL)	0.25	29.4	26.6	6.30	9.17
	0.5	32.6	19.0	6.46	9.62
	0.75	32.1	22.8	7.01	9.63
Packing Sequence (KL ---> Y)	0.25	30.0	23.6	6.26	9.19
	0.5	32.0	23.2	6.96	9.71
	0.75	32.3	21.2	7.01	9.82
Pure KL	1	25.2	29.3	5.44	7.72

**Table 4.4** Pyrolysis product obtained from different packing styles of Pt/Y and Pt/KL zeolites

Case		Product Yield		Yield of Light Olefins (g/100 g Tire)	Yield of Cooking Gas (g/100 g Tire)
Catalyst	$\emptyset_{Pt/KL}$	Gas (%)	Liquid (%)		
Pt/Y	0	29.0	23.5	6.09	8.77
Physical Mixture (Pt/Y + Pt/KL)	0.25	28.4	27.7	6.02	8.83
	0.5	30.0	26.1	6.27	9.38
	0.75	22.6	33.0	4.84	6.97
Packing Sequence (Pt/Y $\rightarrow$ Pt/KL)	0.25	24.2	33.3	5.08	8.15
	0.5	27.4	28.7	5.78	8.40
	0.75	29.6	26.8	6.69	9.17
Packing Sequence (Pt/KL $\rightarrow$ Pt/Y)	0.25	29.8	27.3	6.26	9.54
	0.5	30.4	26.5	6.55	9.86
	0.75	27.4	24.7	5.79	8.04
Pt/KL	1	24.6	28.3	5.40	7.74

According to the ratio ( $\alpha_i$ ) for pyrolysis products, the two regions can be identified in terms of the performance of platinum on pyrolysis products constituents as follows. The first region ( $\alpha_i > 1$ ) represents the case when the performance of a platinum loaded-catalyst is higher than the corresponding non-platinum loaded one. The second region ( $\alpha_i < 1$ ) is where the performance of a platinum loaded-catalyst is lower than the corresponding non-platinum loaded one. The third region ( $\alpha_i = 1$ ), is where the performance of a platinum loaded-catalyst is comparable with the corresponding non-platinum loaded one.

Figure 4.13 shows the  $\alpha$  value of the gas to oil ratio. The results indicate that platinum loading has the negative influence on the product yields. The  $\alpha_{G/L}$  values of the three packing cases are lower than 1.

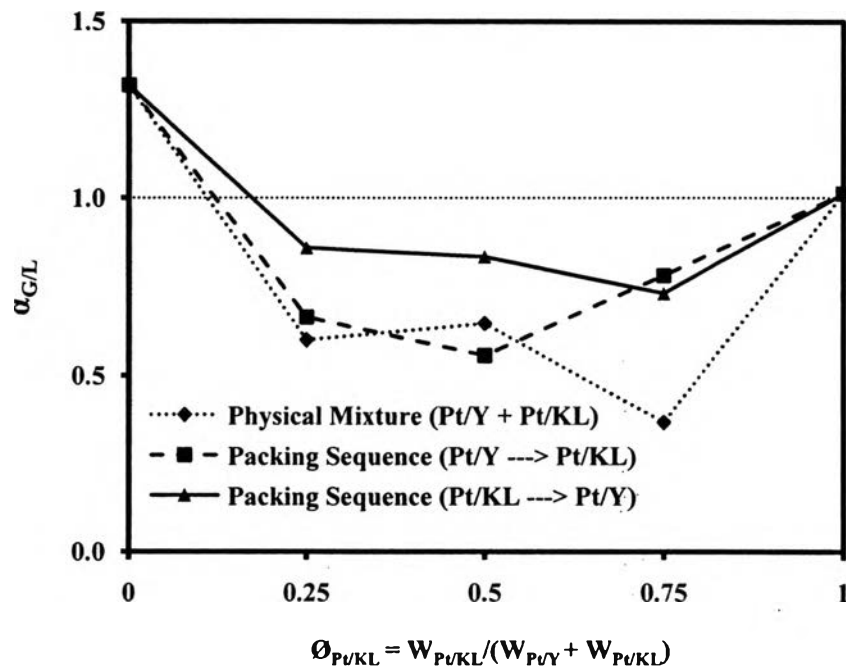


**Figure 4.13** The  $\alpha_{G/L}$  at different styles of double bed packing and various weight fractions of KL.

#### 4.3.2 Gas composition

##### 4.3.2.1 Light Olefin and Cooking Gas Production

Figures 4.14 and 4.15 illustrate the influence of double-bed catalysts with platinum loading on light olefins and cooking gas productions, respectively. In this research, the light olefins mean ethylene and propylene, and the cooking gas is the mixed gas of propane and C<sub>4</sub>s. The results show that  $\alpha_{\text{light olefins}}$  is lower than one, except Pt/Y. For  $\alpha_{\text{Cooking gas}}$ , the results also show the same trend as compared to the light olefins production. Platinum loading makes the  $\alpha_{\text{Cooking gas}}$  value  $< 1$  for the case of the physical mixing (Y + KL) and the packing sequence (Y  $\rightarrow$  KL). On the other hand, loading platinum in the case of packing sequence (KL  $\rightarrow$  Y) at the  $\phi_{KL} = 0.25$  and  $\phi_{KL} = 0.5$  gives the  $\alpha_{\text{Cooking gas}}$  value  $> 1$  (Figure 4.14).

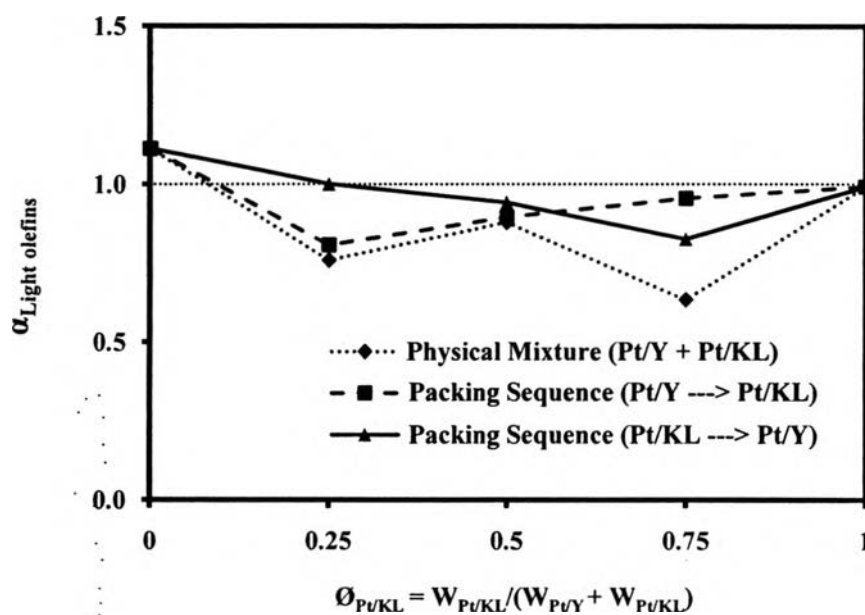


**Figure 4.14** The  $\alpha_{\text{light olefins}}$  at different packing sequences and various weight fractions of KL.

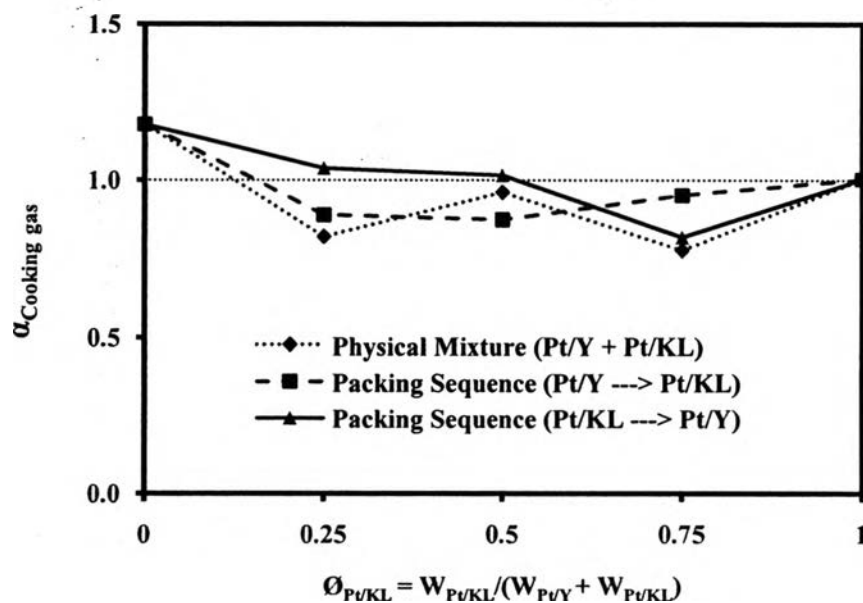


**Figure 4.15** The  $\alpha_{\text{cooking gas}}$  at different packing sequences and various weight fractions of KL.

### 4.3.3 Oil Products

Tables 4.5 and 4.6 demonstrate the petroleum fraction and chemical composition in maltene without and with platinum loading, respectively. The ratio ( $\alpha_i$ ) is also applied in this section.

**Table 4.5** Petroleum fractions and chemical compositions in the liquid products obtained from the different packing styles of Y and KL zeolites

Case		Petroleum Fraction			Chemical Composition	
Catalyst	$\emptyset_{KL}$	Naphtha (%)	Kerosene (%)	Gas Oil (%)	Saturated Hydrocarbons (%)	Total Aromatics (%)
Pure Y	0	25.5	36.0	32.5	54.5	45.3
Physical Mixture (Y + KL)	0.25	40.0	28.0	26.0	67.9	29.0
	0.50	34.0	29.0	31.0	62.2	34.8
	0.75	48.0	25.0	23.0	60.0	39.0
Packing Sequence (Y ---> KL)	0.25	40.0	24.0	29.0	60.9	38.6
	0.50	44.0	23.0	26.0	53.0	45.5
	0.75	40.0	25.0	30.0	54.4	44.7
Packing Sequence (KL ---> Y)	0.25	39.0	26.0	28.0	52.2	44.7
	0.50	37.0	27.0	29.0	43.7	51.9
	0.75	39.0	24.0	30.0	49.0	48.5
Pure KL	1	27.0	39.0	29.5	53.1	44.5

**Table 4.6** Petroleum fractions and chemical compositions in the liquid products obtained from the different packing styles of Y and KL zeolites with platinum loading

Case		Petroleum Fraction			Chemical Composition	
Catalyst	$\emptyset_{P/KL}$	Naphtha (%)	Kerosene (%)	Gas Oil (%)	Saturated Hydrocarbons (%)	Total Aromatics (%)
Pt/Y	0	47.0	23.0	25.0	55.4	42.1
Physical Mixture (Pt/Y + Pt/KL)	0.25	38.5	27.0	29.0	69.7	30.0
	0.50	48.0	24.5	23.0	68.0	29.0
	0.75	37.0	28.0	30.0	67.3	26.0
Packing Sequence (Pt/Y ---> Pt/KL)	0.25	33.0	26.0	34.0	71.0	27.0
	0.50	40.0	20.5	33.5	76.1	23.4
	0.75	43.0	24.0	27.0	68.5	30.6
Packing Sequence (Pt/KL ---> Pt/Y)	0.25	43.0	25.0	27.0	76.2	23.3
	0.50	43.0	24.0	27.0	69.1	30.6
	0.75	44.0	24.0	27.0	59.3	38.2
Pt/KL	1	49.0	28.0	19.5	55.5	42.9

Figures 4.16–4.18 show roughly the quality of three main petroleum products obtained from various styles of packing. In this section, the oil products are presented in terms of  $\alpha_{\text{Naphtha}}$ ,  $\alpha_{\text{Kerosene}}$ , and  $\alpha_{\text{Gas oil}}$ , respectively. Figure 4.16 shows that the  $\alpha_{\text{Naphtha}}$  values of Pt/Y, Pt/KL, and the packing sequence (Pt/KL ---> Pt/Y) are higher than 1. Figure 4.17 shows the  $\alpha_{\text{kerosene}}$  values of the all packing cases are below 1. In contrast, Figure 4.18 shows that the  $\alpha_{\text{Gas oil}}$  values of the physical mixture (Pt/Y + Pt/KL) and the packing sequence (Pt/Y ---> Pt/KL) are higher than 1.

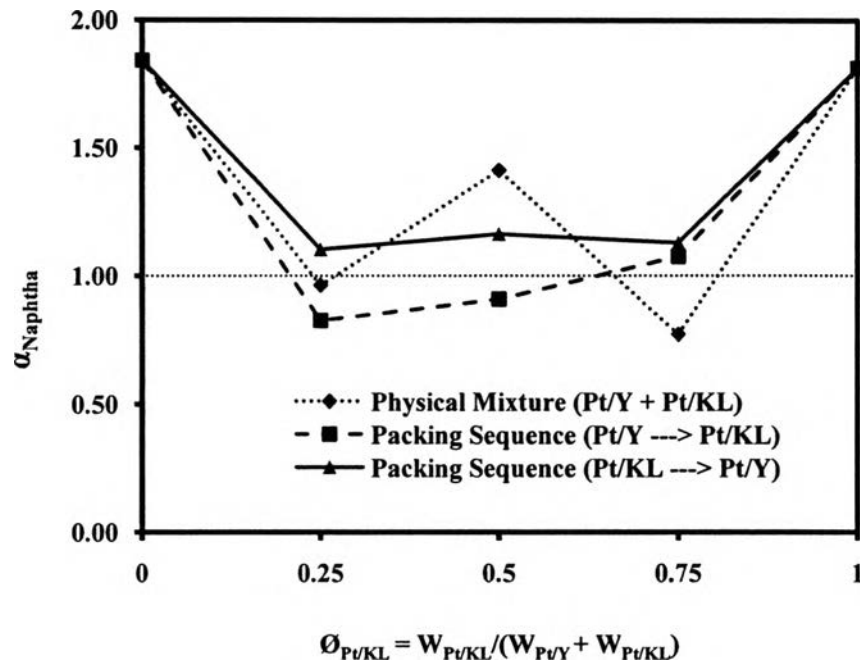


**Figure 4.16** The  $\alpha_{Naphtha}$  obtained from different packing styles at various weight fractions of KL.

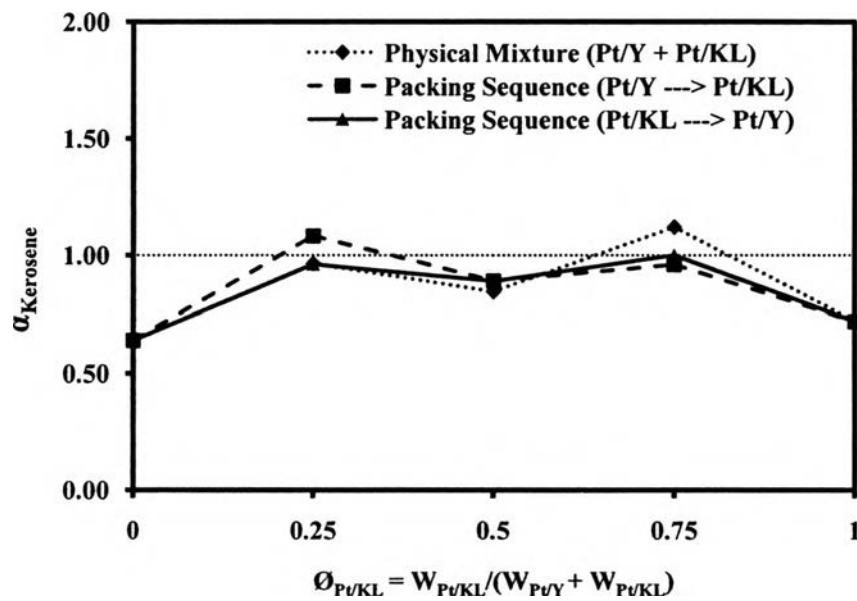


**Figure 4.17** The  $\alpha_{Kerosene}$  obtained from different packing styles at various weight fractions of KL.



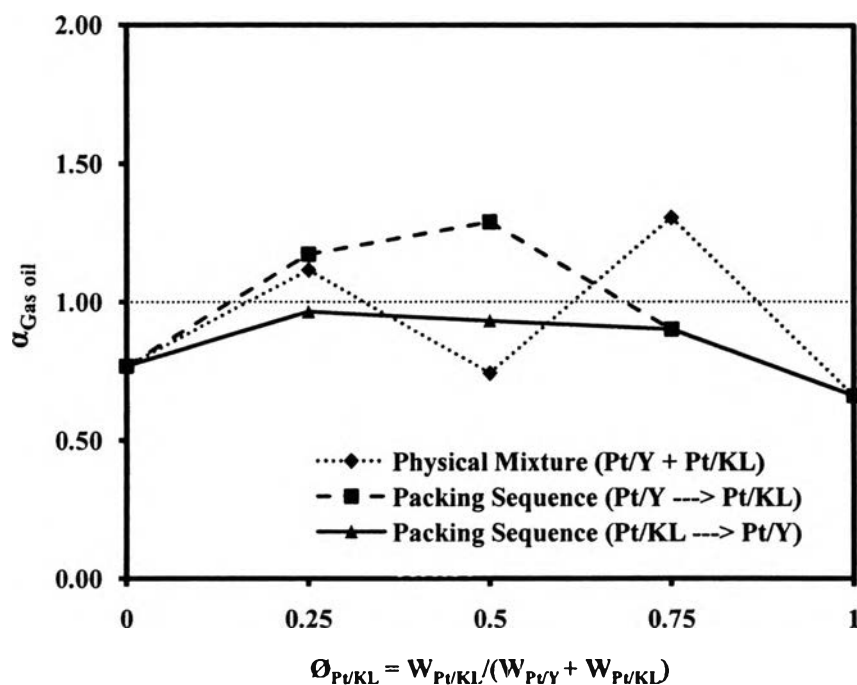


**Figure 4.18** The  $\alpha_{\text{Gas oil}}$  obtained from different packing styles at various weight fractions of KL.

Figures 4.19–4.20 demonstrate the  $\alpha$  values of saturated hydrocarbon and total aromatic compounds, respectively. In the presence of platinum, the  $\alpha_{\text{saturated hydrocarbons}}$  values of the all packing cases are higher than 1. Moreover, all platinum catalysts can also reduce  $\alpha_{\text{Total aromatic hydrocarbons}} (<1)$ . The packing sequence (Pt/KL ---> Pt/Y) at  $\phi_{Pt/KL} = 0.5$  can tremendously produce saturated hydrocarbon up to 2.2 times, and reduce total aromatics about 0.78 times as much as the corresponding non-platinum loading cases. In addition, the total aromatic hydrocarbons are also highly reduced (about 0.6 times lower than the non-platinum loading cases) in the case of Pt/KL ---> Pt/Y at  $\phi_{Pt/KL} = 0.25$ .

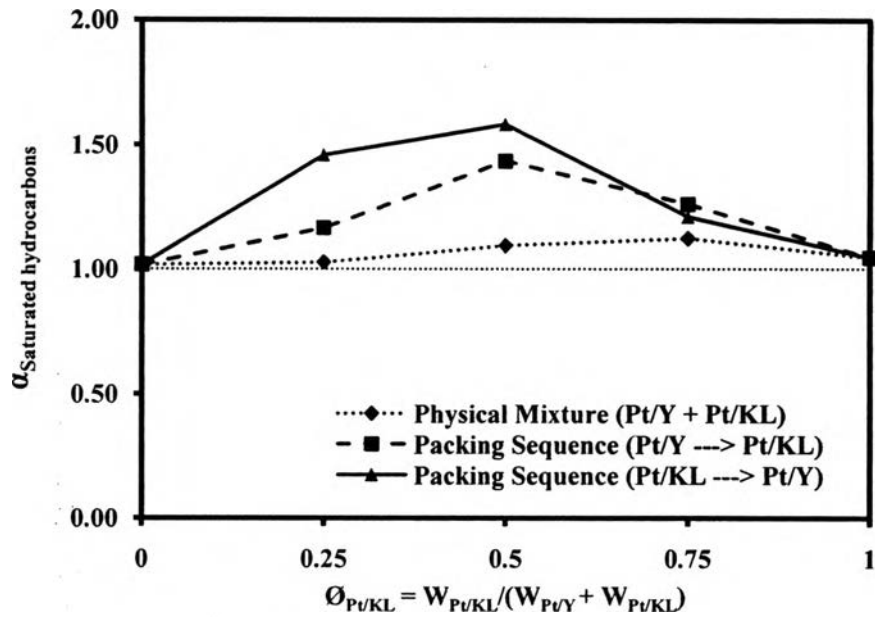


**Figure 4.19** The  $\alpha_{\text{Saturated hydrocarbons}}$  obtained from different packing styles at various weight fractions of KL.

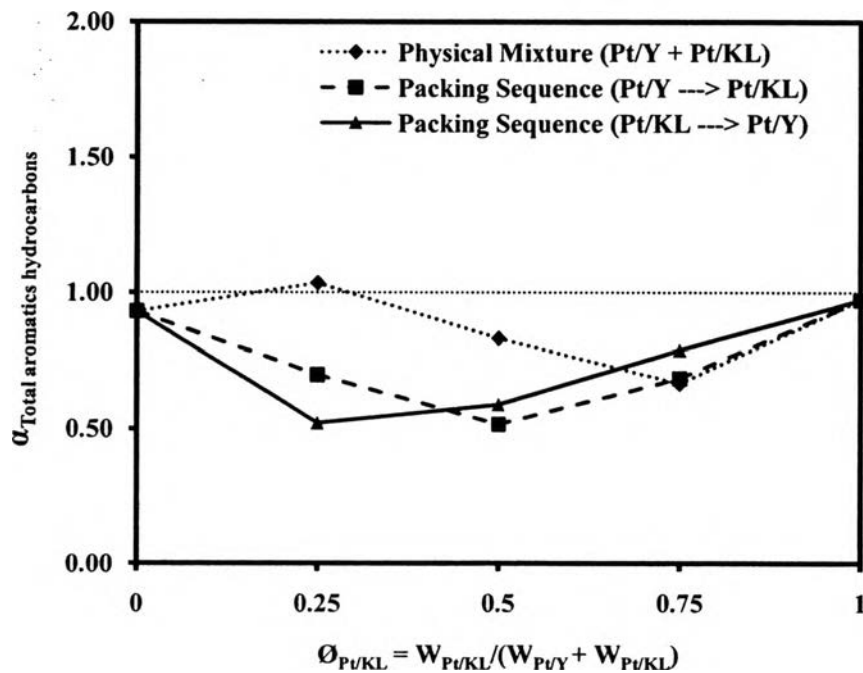


**Figure 4.20** The  $\alpha_{\text{Total aromatic hydrocarbons}}$  obtained from different packing styles at various weight fractions of KL.

Figure 4.21 shows the asphaltene reduction in oil product. It can be observed that Pt loading for the packing sequence cases provide  $\alpha_{\text{Asphaltene}} < 1$ . However, the platinum loaded on the physical mixture case provides the lower asphaltene in the oil product than without platinum, except at  $\phi_{\text{Pt/KL}} = 0.25$  which gives  $\alpha_{\text{Asphaltene}} > 1$ .

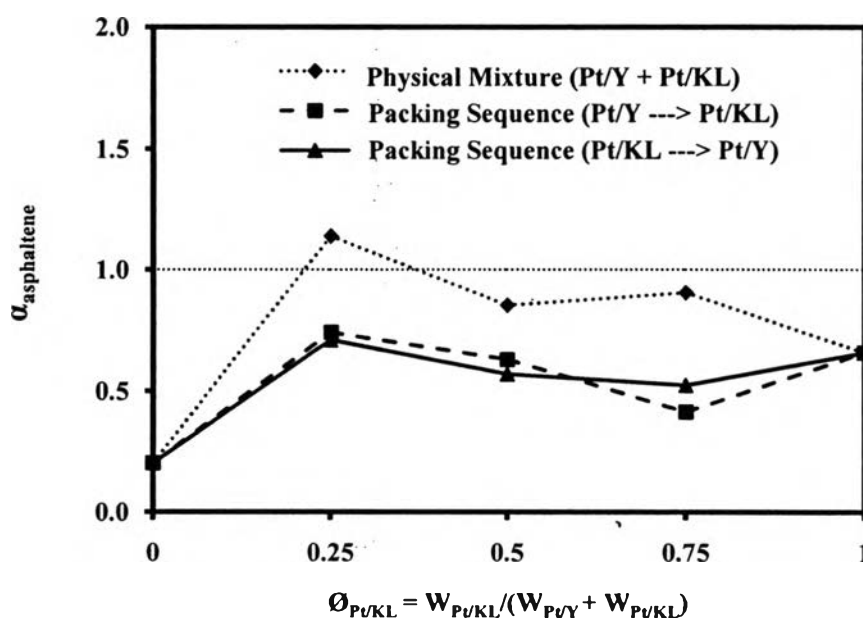


**Figure 4.21** The  $\alpha_{\text{asphaltene}}$  at different packing sequences and various weight fractions of KL.

#### 4.3.4 Coke and Sulfur Formation

The  $\alpha$  values of coke formation and sulfur deposition on the catalysts are shown in Table 4.7. The results show that most of spent catalysts show the same trend in the both cases of  $\alpha_{\text{coke}}$  and  $\alpha_{\text{sulfur}}$ . Especially, the packing sequences (Pt/Y ---> Pt/KL and Pt/KL ---> Pt/Y) show  $\alpha_{\text{coke}}$  and  $\alpha_{\text{sulfur}} > 1$  on the Pt/Y layer. It may be due to the highest acid strength of Pt/Y, resulting in the high amount of coke and sulfur deposited on Pt/Y. For the case of physical mixtures, the  $\alpha_{\text{coke}}$  and  $\alpha_{\text{sulfur}}$  values are lower than 1. It probably means that the interaction between the strong acid sites and the small clusters of platinum metal results in the electrons being withdrawn from the noble metal; thus, creating an electron-deficient metal particle. This cause can decrease the strength of the bonding interaction between sulfur and

metal (Choosuton, 2007). Hence, sulfur is splitted-over to acid sites and might associate with the increasing total aromatic compounds as shown in Figure 4.20. In addition, the Pt/KL gives  $\alpha_{\text{coke}}$  and  $\alpha_{\text{sulfur}} > 1$ . Jacob *et al.*, 1998 studied the n-hexane aromatization on Pt/KL in the sulfur-containing feeds. They reported that the deactivation was evident not only in the overall conversion but also in benzene selectivity. After the n-hexane aromatization reaction, the carbon deposits on Pt/KL. That is why the amount of coke is increased when the platinum is loaded on KL zeolite.

**Table 4.7** Coke and sulfur formation from the different packing styles with platinum loading

Catalyst	$\emptyset_{\text{KL}}$	Layer	$\alpha_{\text{coke}}$	$\alpha_{\text{sulfur}}$
Pt/Y	0	-	0.86	1.47
Physical Mixture (Pt/Y + Pt/KL)	0.25	-	0.79	0.73
	0.5	-	0.89	0.83
	0.75	-	0.75	0.71
Packing Sequence (Pt/Y ---> Pt/KL)	0.25	KL	0.94	0.80
		Y	1.36	1.75
	0.5	KL	0.85	0.84
		Y	1.01	1.10
	0.75	KL	0.80	0.84
		Y	0.96	0.90
Packing Sequence (Pt/KL ---> Pt/Y)	0.25	Y	1.02	1.05
		KL	1.07	1.26
	0.5	Y	1.17	1.19
		KL	0.81	0.72
	0.75	Y	0.99	0.96
		KL	1.02	0.71
Pt/KL	1	-	1.16	1.05

In summary, the case of physical mixtures (Pt/Y + Pt/KL), the  $\alpha_{\text{GL}}$ ,  $\alpha_{\text{Light olefins}}$ ,  $\alpha_{\text{Cooking gas}}$ , and  $\alpha_{\text{Naphtha}}$ , and  $\alpha_{\text{Naphtha}}$  are lower than 1. However, the  $\alpha_{\text{saturated hydrocarbons}}$  are higher than 1. It can be suggested that the surface activity of

the double bed catalysts is decreased by platinum occupation. The results are similar to Kumar *et al.*, 2008, who suggested that the performance of catalysts was affected by the change in acidity or basicity of the support that governs the platinum agglomeration on the support. Therefore, the cracking activity of all double-beds catalysts with platinum loading are lowered. It implies that the platinum metal loaded on zeolites is not suitable for gas production.

Moreover, the packing sequences (Pt/Y  $\rightarrow$  Pt/KL and Pt/KL  $\rightarrow$  Pt/Y) and the single Pt/KL bed give  $\alpha_{\text{coke}} > 1$ , while the physical mixtures give the  $\alpha_{\text{coke}} < 1$ . As supported by Choosuton (2007), it was shown that only 0.65 and 0.98 times of ethylene and cooking gas production using Pt/USY catalyst were obtained as compared to the non-catalyst pyrolysis. Moreover, Pt makes coke or/and complex containing sulfur grow more rapidly on the surface of catalyst, resulting in deactivation and then increase in liquid yield (see Table 4.7). Lin *et al.* (1997) showed that the USY activity declined exponentially with coke content. The catalyst then lost approximately half of its activity with the coke content of 4.24%. In the case of sulfur formation, the packing sequences (Pt/Y  $\rightarrow$  Pt/KL and Pt/KL  $\rightarrow$  Pt/Y) and the single Pt/KL bed give  $\alpha_{\text{sulfur}} > 1$ , while the physical mixtures give the  $\alpha_{\text{sulfur}} < 1$ . Therefore, loading with Pt enhances sulfur deposition. Jongpatiwut *et al.* (2002) found that the presence of sulfur not only inhibited hydrogenolysis, but also the aromatization activity. And the effect of coke alone results in the rapid decrease in activity of the catalysts. (Jacobs *et al.*, 1998). That is why the yields to cooking gas, light olefins, and naphtha fraction are decreased when the platinum is loaded on the physical mixture case (see Figures 4.14, 4.15, and 4.16).

In the case of Pt/Y  $\rightarrow$  Pt/KL, the  $\alpha_{\text{Gas oil}}$  is higher than 1. It can be explained that in the presence of Pt/KL, the dehydrocyclization of small molecules such as alkanes are occurred resulting in the production of heavy aromatic hydrocarbons. Fang *et al.*, 1997 supported that Pt/KL was very beneficial to the aromatic selectivity as well as beneficial to decrease the hydrocracking selectivity in aromatization of  $C_6$  feed stock. And, they explained that the platinum function alone could catalyze aromatics formation by cyclization and subsequent dehydrogenation to aromatics. Otherwise, the high amount of coke formation, partial pore blocking

occurs, so that the acidity of external surface of catalyst is decreased resulting in the lower yield to naphtha fraction when compared with non-platinum loading. However, these can be also described by the cracking of the chain of heavy molecules such as naphtha and kerosene to lighter products where the vacuum gas oil could be formed from the recombination of cracked molecules of naphtha and kerosene (Meng *et al.*, 2006). Moreover, the  $\alpha$  values of saturated hydrocarbon are higher than 1, because the introduction of platinum on KL zeolites leads to a hydrogenation in fraction of unsaturated hydrocarbons. In 1999, Jacobs *et al.* studied the influence of platinum particle morphology on aromatization activity and deactivation. They found that the higher loading of Pt over KL zeolite exhibited significantly higher 3-methylpentane/2-methylpentane ratio on MPC ring opening as compared to the low loading IWI catalyst.

In the case of Pt/KL  $\rightarrow$  Pt/Y, the  $\alpha_{\text{Cooking gas}}$  is higher than 1 at  $\phi_{\text{Pt/KL}}$  at 0.25 and 0.5. It can be explained that the first layer of Pt/KL enhances the hydrogenation of the thermal cracking products, followed by hydrocracking in the second layer by Pt/Y. Thus, the yields of cooking gas in the Pt/KL  $\rightarrow$  Pt/Y case at the  $\phi_{\text{KL}} = 0.25$  and  $\phi_{\text{KL}} = 0.5$  are the highest among those obtained from three packing cases. Moreover, there have been many researchers reported that Pt/KL zeolite is very selective to aromatics from the conversion of light naphtha while a twelve ring pore zeolite, such as Y supported platinum, can enhance the bimolecular alkylation reactions, which lead to the formation of aromatics (Smirniotis and Ruckenstein, 1995). Park and Ihm (2000) explained that the isomerization selectivity can be improved by suppressing hydrocracking. One possible way is to use the shape-selectivity of zeolites (Pt/Y) for suppressing the formation of multibranched isoalkane, which is susceptible to hydrocracking. Pt/KL  $\rightarrow$  Pt/Y also shows  $\alpha_{\text{Naphtha}} > 1$ . It can be described that the catalytic cracking reaction occurs so that the chains of heavy molecules break down to lower molecular weight product, such as naphtha fractions. Or, these could be attributed to the high hydrogenolysis of platinum that helps cracking of the heavy molecules to small molecules. Besides, the hydrogenated compounds (Pt/Y) might further cracking and the converting to lighter fractions. Trakarnroek *et al.*, 2007 explained that the diffusion of o-xylene was slower than that of ethylbenzene and it was easily converted to smaller molecules such as benzene,

toluene, and methane by the secondary hydrogenolysis of Pt/KL. Moreover, Pt/HY showed a high ring opening conversion resulting in the large amount of naphthenic ring cleavage and C<sub>2+</sub> n-alkane formation. These results were also reported by Castaño *et al.*, 2006. In the case of saturated hydrocarbons, the  $\alpha$  values are higher than 1. It can be explained that Pt loaded on Y zeolite in the second layer case can enhance the hydrogenation and ring opening reaction of aromatic compounds, resulting in the production of saturated hydrocarbons, much more effective than the other packing styles. Similar results were reported by Santikunaporn *et al.*, (2004) who studied the ring opening of naphthenic rings to produce molecules of higher cetane numbers on Pt/HY. They found that the production of ring opening products was greatly enhanced by the presence of platinum. Arribas and Martínez (2002) studied the influence of zeolite acidity for coupled hydrogenation and ring opening of 1-methylnaphthalene on Pt/USY. They found that the selective ring opening of 1-methylnaphthalene was favored over zeolites with a low density of Brønsted acid site. Dũng *et al.*, 2009 explained that the high hydrogenation activity of platinum that helped converting olefins and other unsaturated intermediates to saturated hydrocarbon.

For asphaltene, it is possible that the two packing sequences (Pt/Y  $\rightarrow$  Pt/KL and Pt/KL  $\rightarrow$  Pt/Y) might further promote cracking reaction over acid sites by hydrogenation. Thus, the heavy molecules are cracked into lighter compound, resulting in the increase in naphtha fraction (Figure 4.16). Furthermore, using bifunctional catalysts, the products adsorb over a Brønsted acid site or a strong Lewis acid site of acid catalyst, forming a carbenium ion, and then the carbenium ion moves to a metal site to be hydrogenated producing a saturated product. In the case of Pt/KL packed in the second layer, the main reaction is ring opening catalyzed by the active metal. Next, the products can be converted to the small molecules (Aboul-Gheit *et al.*, 2005).